Galaxy Groups and Clusters

One major difficulty with group/cluster identifications is the conversion of velocity to distance. In general, this is done via the adoption of a Hubble Constant. However,

- Peculiar velocities can affect distance measurements by typically ~ 4 Mpc
- Galaxy clusters can have a large velocity dispersion. This creates a "finger of God" effect, where the galaxies appear to line up along the line of sight.
- The Hubble flow of large superclusters may just now start to reverse. This can cause the galaxies to appear flat against the sky.

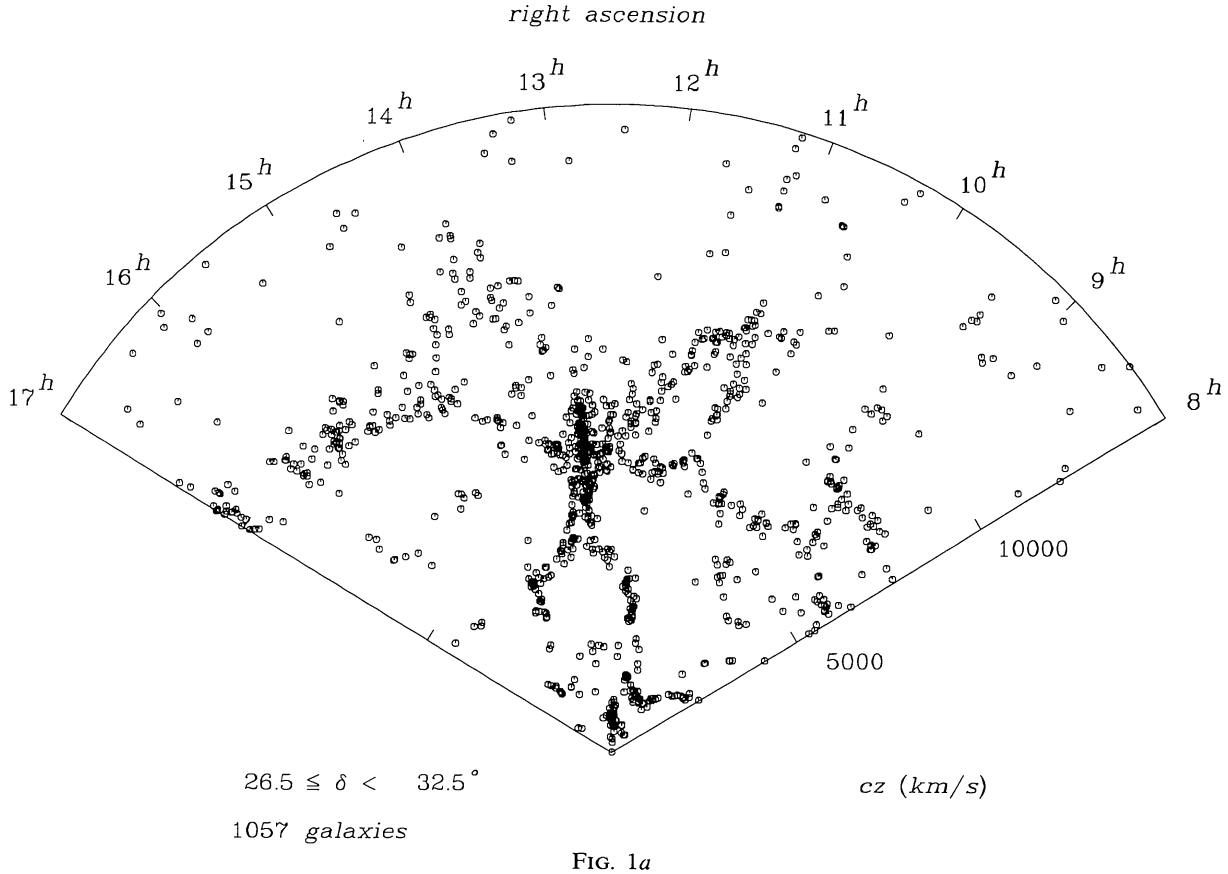

FIG. 1*a*

[Huchra *et al.* 1990, *Ap.J. Supp.*, **72,** 433]

Group/Cluster Definitions

[Huchra & Geller 1982, *Ap.J.,* **257,** 423]
[Nolthenius & White 1987, *MNRAS,* **235,** 505]
[Yang *et al.* 2005, *MNRAS,* **356,** 1293]

The traditional approach to defining a galaxy group is the percolation, or friends of friends approach. Simply put, any galaxy that is within a distance r of another galaxy is a member of that galaxy's group. So if galaxy A is close to galaxy B, and galaxy B is close to galaxy C, then A, B, and C are all members of the same system. This definition is straightforward, but it depends critically on the connection length, r.

A second method is to define a group as a region where the density enhancement of galaxies is a factor of n above the background. One can use the friends of friends approach to create an initial catalog, and then use the density enhancement criteria (over some assumed shape) to define r.

A completely different method invokes the results of CDM cluster simulations, and models of heirarchical cluster formation. One first assumes a mass-to-light ratio, and tentatively defines group membership (perhaps with a friends of friends approach). One then uses the total group luminosity and the mass-to-light ratio to estimate the group's mass. Once this is done, the halo occupancy predictions of CDM models are used to estimate the group's size, and therefore its velocity dispersion. Finally, the derived velocity dispersion is compared to the observed dispersion, and group members are added or subtracted to improve agreement. The process is then repeated until the group definition converges.

Virgo and the Virgocentric Flow

[Huchra 1988, ASP Conf. 4, The Extragalactic Distance Scale, 257]
[Binggeli, Tammann, & Sandage 1987, *A.J.*, **94**, 251]

The dominant system in the Local Supercluster is the Virgo Cluster. However, it is not a relaxed system it can be divided into numerous subsystems.

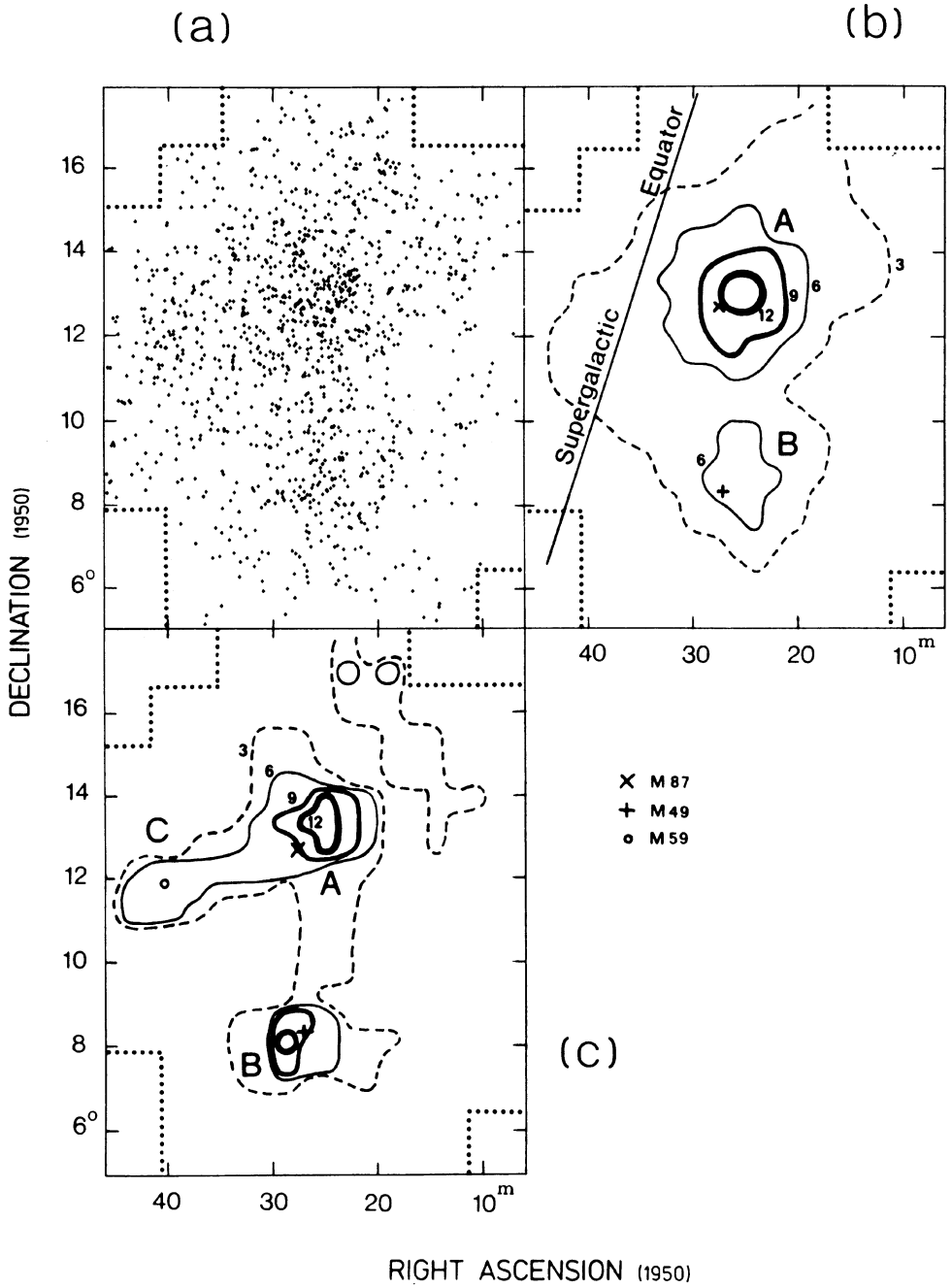

FIG. 4. General outline of the Virgo cluster, based on all cluster members listed in the Virgo Cluster Catalog. (a) Plot of all members. (b) Isopleths based on number counts in cells of size $0.^{\circ}5 \times 0.^{\circ}5$, smoothed by averaging over $1.^{\circ}5 \times 1.^{\circ}5$. The contours are labeled in units of galaxies per cell, i.e., number of galaxies per 0.25 square degree. (c) Same as (b) but with luminosity-weighted isopleths, labeled in units of $10^{10}\ L_{\odot}$ per deg^2.The positions of M87, M49, and M59, which are associated with the three major clumps A (M87 cluster in Fig. 1), B (M49 cluster), and C are indicated. For orientation, the position of the supergalactic equator is given in (b).

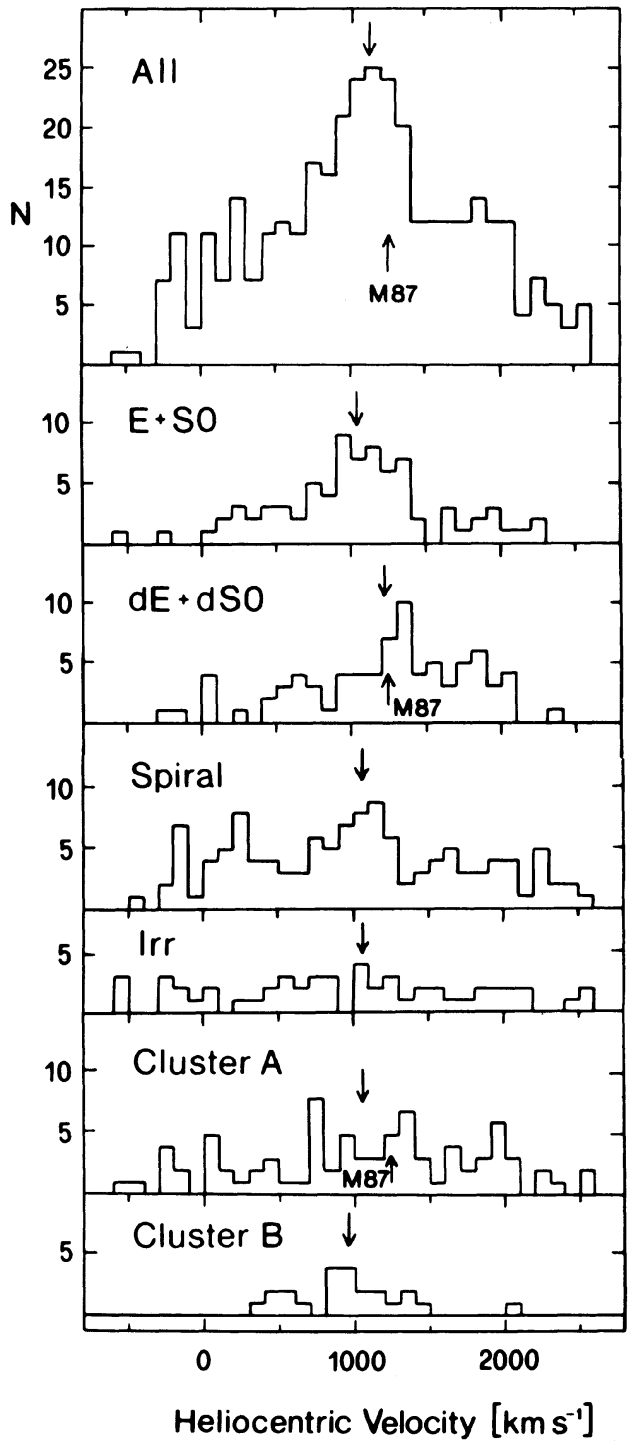

FIG. 23. Velocity distribution for the entire Virgo cluster sample broken up into four different morphological groups, and into galaxies of all types in the areas of cluster A (around M87) and cluster B (around M49), defined by the two contours labeled "6" in Fig. 4(b). The arrows pointing downwards mark the corresponding velocity means, which are also listed in Table IV. For comparison, the velocity of M87 is indicated by an arrow pointing upwards.

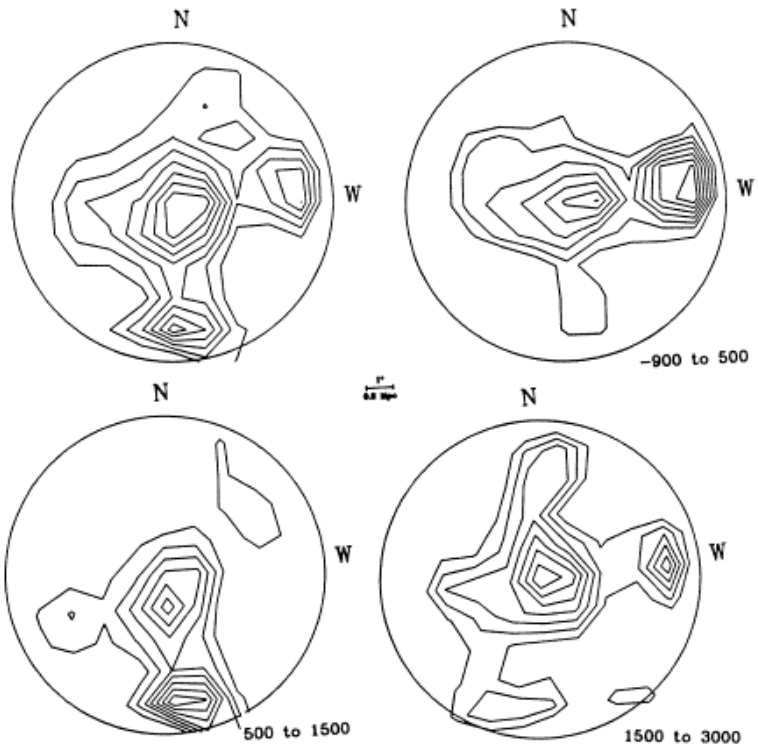

Figure 8. Surface distribution of (a) all galaxies with velocities $\leq$ 3000 km s^{-1}in the Virgo core, (b) the same for those galaxies with velocities less than 500 km s^{-1}, (c) galaxies between 500 and 1500 km s^{-1}, and (d) galaxies with velocities between 1500 and 3000 km s^{-1}. The clumpy nature of the cluster core is easily seen. (From Huchra 1985).

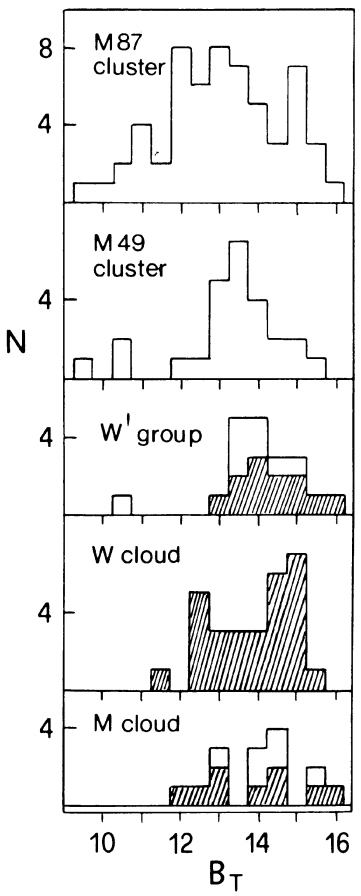

FIG. 2. Differential luminosity functions for the five concentrations appearing in Fig. 1. All E + S0 + Spiral galaxies within each circle in Fig. 1 are counted; dwarf galaxies (as classified in the Catalog) are not included. Open histograms refer to galaxies classified as members in Paper II, hatched histograms to possible members.

The Virgocentric Flow

[Aaronson *et al.* 1982, *Ap.J.*, **258, 64**]

The infall of galaxies towards Virgo dominates galactic motions in the Local Supercluster. As illustrated by this apple diagram, in some directions, the radial velocities of galaxies are tripled-valued.

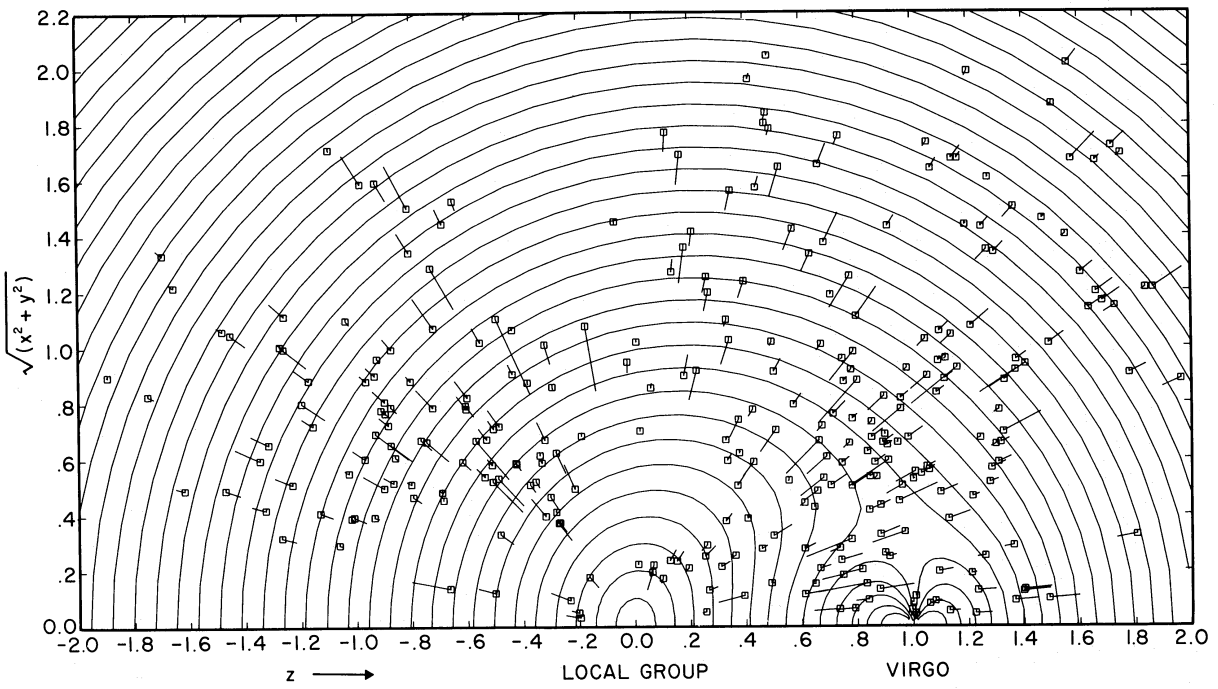

FIG. 3.—Normalized redshift residuals for solution 1, roughly log v_{pred} − log v_{obs}, with positive residuals pointing away from the position of the Local Group at $z = 0$. Galaxies are plotted on a meridional plane, with positions inferred from H I velocity widths. Contours show predicted redshifts, uncorrected for the peculiar motion of the Local Group, spaced at intervals 1/10 the Virgo redshift (after correction for our peculiar z velocity).

Large Scale Bulk Flows

[Tonry *et al.* 2000, *Ap.J.*, **530,** 625]

The Local Group is moving towards Virgo ($b^{II} = 74°$, $l^{II} = 283°$) at a velocity of ~ 270 km s^{-1}; this is called the "Virgocentric Infall." However, when one measures the anisotropy in the microwave dipole radiation, the absolute motion of the Milky Way is ~ 620 km s^{-1} in the direction of $b^{II} = 27°$, $l^{II} = 268°$. This is presumably due to the potential of the Hydro-Centaurus Supercluster (once known as the Great Attractor). Unfortunately, the center of this supercluster lies in the Galactic plane, so it is difficult to study.

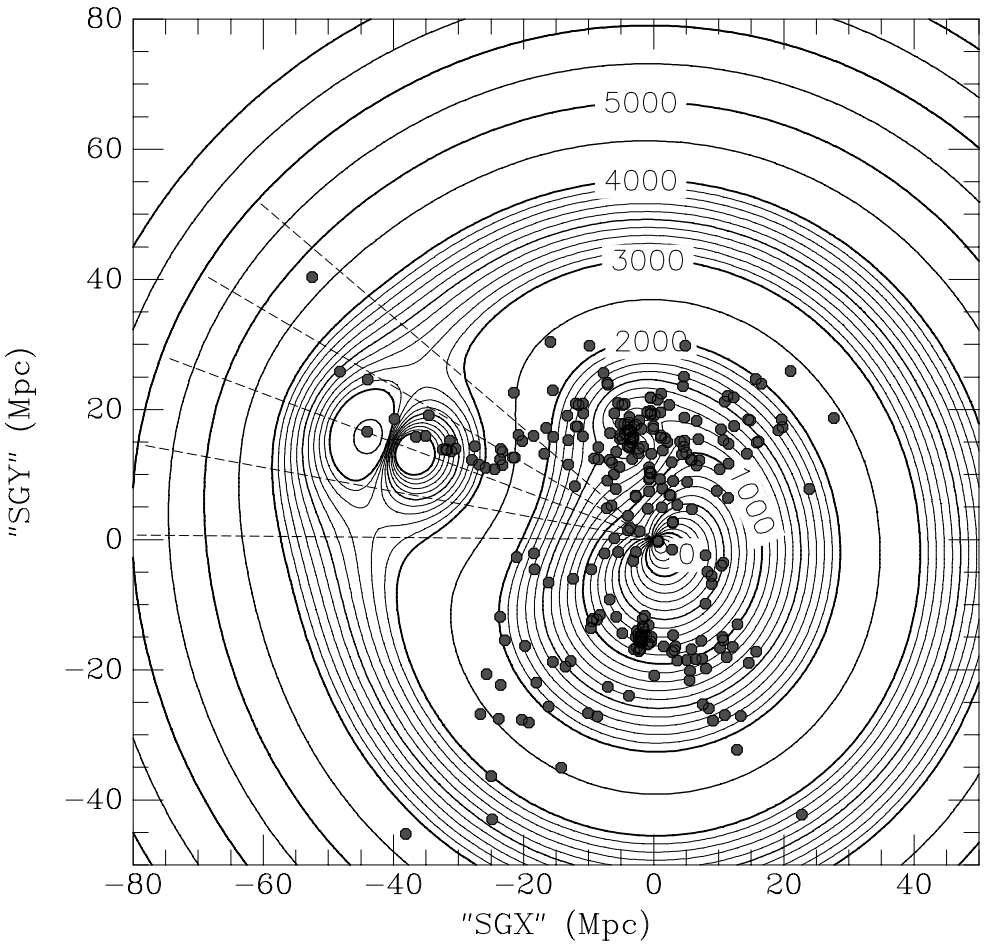

FIG. 21.—Same as Fig. 20, except that our survey galaxies are overplotted. Note that the Centaurus galaxies that appear to be going through the Great Attractor actually pass above it by about 15°, and hence, lie in the stall zone.

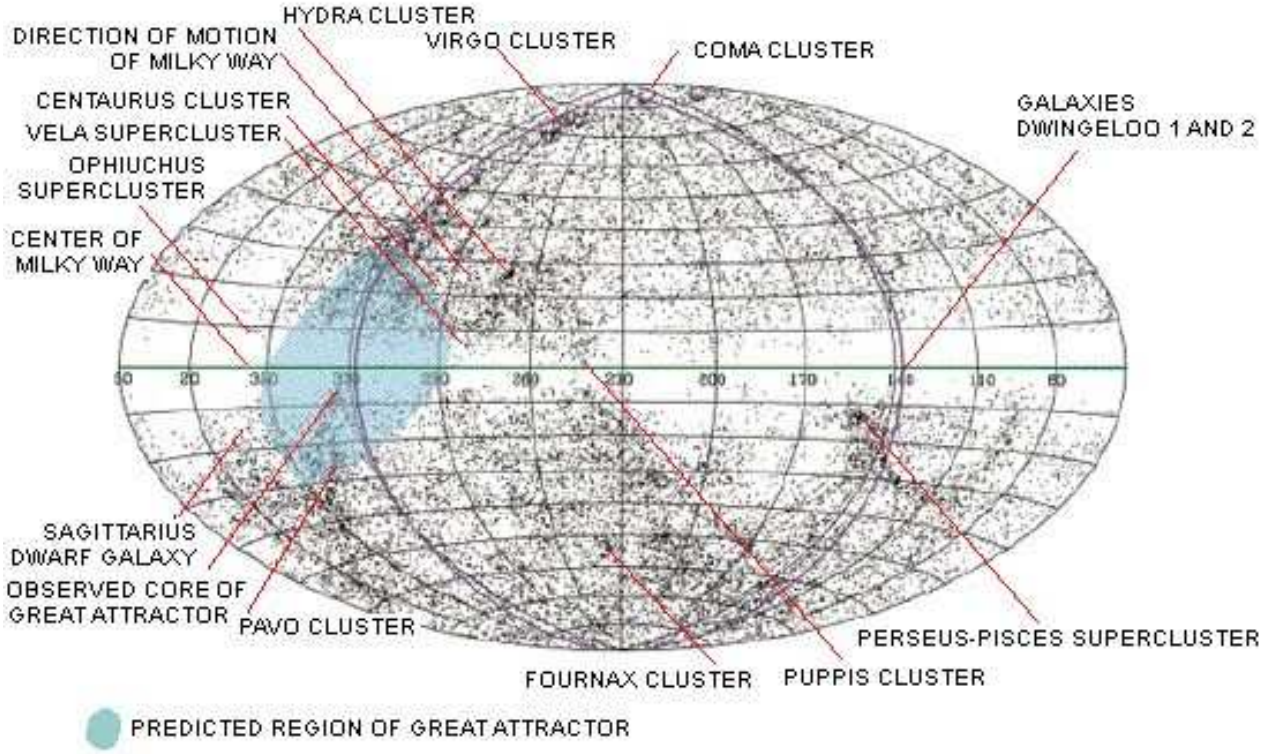
HYDRA CLUSTER
DIRECTION OF MOTION OF MILKY WAY
VIRGO CLUSTER
COMA CLUSTER
CENTAURUS CLUSTER
VELA SUPERCLUSTER
OPHIUCHUS SUPERCLUSTER
CENTER OF MILKY WAY
GALAXIES DWINGELOO 1 AND 2
SAGITTARIUS DWARF GALAXY
OBSERVED CORE OF GREAT ATTRACTOR
PAVO CLUSTER
PERSEUS-PISCES SUPERCLUSTER
FOURNAX CLUSTER
PUPPIS CLUSTER
PREDICTED REGION OF GREAT ATTRACTOR

The Two-Point Correlation Function

The most common way of describing the overall clustering of galaxies is through the two-point correlation function. This can be performed either on the projected distribution of galaxies on the sky (the 2-D case) or the 3-D galaxy distribution.

The premise of the two-point correlation function is simple. If galaxies are Poissonly distributed, the number of galaxies you can expect to find in a volume dV_1 is

$$dN_1 = \rho_0 dV_1 \tag{23.01}$$

where ρ_0 is the average density of galaxies in the entire volume. (If dV_1 is infinitessimal, then this number is a probability, since the chance of finding more than one galaxy in the volume is zero.) Similarly, the probability of finding a galaxy in volume dV_1 and finding another galaxy in volume dV_2 is

$$dN_{\rm pair} = \rho_0^2 dV_1 dV_2 \tag{23.02}$$

We can now define the two-point correlation function, ξ, as the probability of actually observing such a pair of galaxies, compared to the Poisson probability, *i.e.,*

$$dN_{\rm pair} = \rho_0^2 [1 + \xi] dV_1 dV_2 \tag{23.03}$$

where ξ is a function of the separation between the two volume elements, r. In other words, if $\xi(r) > 0$, the positions of the galaxies are correlated; while if $\xi(r) < 0$, the positions are anti-correlated.

Let's look at $\xi(r)$ another way. Let $\delta(x)$ be the relative overdensity of region x, *i.e.,*

$$\delta(x) = \frac{\rho(x) - \rho_0}{\rho_0} \tag{23.04}$$

The probabilty of finding a pair of galaxies in volumes dV_1 and dV_2 centered at positions x_1 and x_2 is

$$\begin{aligned} dN_{\rm pair} &= \rho(x_1)dV_1 \cdot \rho(x_2)dV_2 \\ &= \rho_0 \left\{1 + \delta(x_1)\right\} \cdot \rho_0 \left\{1 + \delta(x_2)\right\} dV_1\, dV_2 \\ &= \rho_0^2 \left\{1 + \delta(x_1)\right\} \left\{1 + \delta(x_2)\right\} dV_1\, dV_2 \\ &= \rho_0^2 \left\{1 + \delta(x_1) + \delta(x_2) + \delta(x_1)\delta(x_2)\right\} dV_1 dV_2 \end{aligned} \tag{23.05}$$

Averaged over the entire field, $\delta(x)$ must equal zero, so

$$dN_{\rm pair} = \rho_0^2 \left\{1 + \delta(x_1)\delta(x_2)\right\} dV_1 dV_2 \tag{23.06}$$

If r is the separation between position x_1 and position x_2, then a comparison of (23.03) and (23.06) yields

$$\xi(r) = \langle \delta(x)\delta(x+r) \rangle = \langle \delta_r^2 \rangle \tag{23.07}$$

In other words, $\xi(r)$ is a measure of the overdensity as a function of radius.

Computing the Two-Point Correlation Function

In order to compute the two-point correlation function, one has to count the number of sources between r and $r + \delta r$ from every object in the catalog, and compare that number to the number you would get from a random distribution.

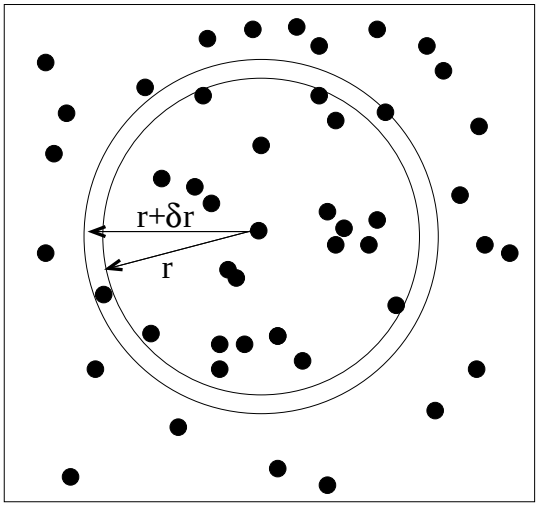

This latter step is tricky. It is usually impossible to estimate the signal of a random distribution analytically: bright stars, changes in the detection threshold (perhaps from extinction), and other factors will effect the "window function" of the observations. In addition, most surveys have edge effects, and objects close to the boundary have fewer neighbors than those near the center. While one can try to compute the correlation function using subsets of data far from the survey boundaries, or do a correction for incomplete shells (Rivolo 1986), most investigators simply perform Monte Carlo experiments. One randomly adds points to the survey area using the exact window function as the original data, and computes

$$\xi(r) = \frac{N_{rd}}{N} \frac{DD(r)}{RR(r)} - 1 \qquad (23.08)$$

where N is the number of data points in the catalog, N_{rd} is the number of random points, $DD(r)$ is the number of pairs with separation r in the data catalog, and $RR(r)$ is the number of pairs with separation r in the random data set. (To minimize

the errors of this procedure, the number of random data points must be many, many times that of the data.)

Unfortunately, this type of procedure still does not remove all the edge effects from the calculation. To remove this bias, a series of improved estimators have been proposed, including one by Davis & Peebles (1983)

$$\xi(r) = \frac{N_{rd}}{N} \frac{DD(r)}{DR(r)} - 1 \tag{23.09}$$

Hamilton (1993)

$$\xi(r) = \frac{DD(r) \cdot RR(r)}{DR(r)} - 1 \tag{23.10}$$

and (currently the most popular) Landy & Szalay (1993)

$$\xi(r) = 1 + \left(\frac{N_{rd}}{N} \right)^2 \frac{DD(r)}{RR(r)} - 2 \frac{N_{rd}}{N} \frac{DR(r)}{RR(r)} \tag{23.11}$$

where $DR(r)$ is the distribution of pair separations in a data versus random point catalog. All these estimators have some bias to them, as they assume a mean density that is defined from the sample data, rather the true, universal mean.

Angular versus Spatial Correlation Functions

Until recently, large extragalactic datasets with full 3-D information (*i.e.,* with redshifts) were rare. Thus, most early analyses involved the angular correlation function, ω. One can infer the three dimensional correlation function from the 2-D function with a little mathematics. Suppose the true 3-D radial distribution of a galaxy cluster with radius R_{max} can be written in the form

$$n(r) = n_0 \left[1 + \xi(r)\right] dV \tag{23.12}$$

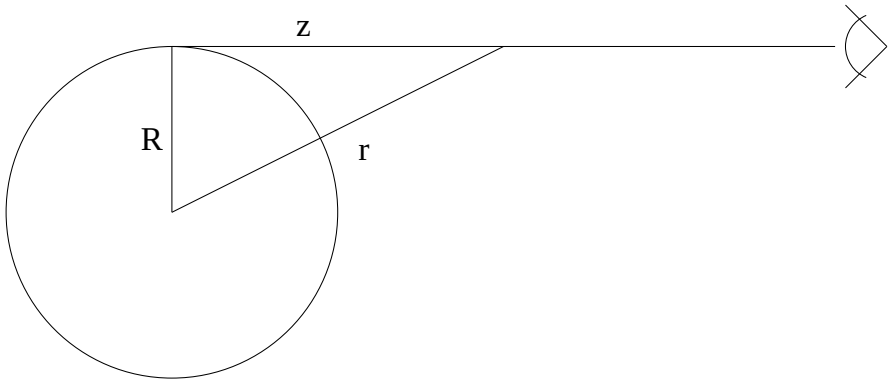

Then, projected on the sky, this distribution will be

$$N(R) = 2\int_R^{R_{max}} \frac{n(r)r}{\left(r^2 - R^2\right)^{1/2}} dr = 2\int_R^{R_{max}} \frac{n_0\left[1 + \xi(r)\right] r}{\left(r^2 - R^2\right)^{1/2}} dr \tag{23.13}$$

where R is the projected distance from the center of the cluster. Now suppose the correlation function can be described as a power law, *i.e.,* $\xi(r) \propto r^{-\gamma}$. Then

$$N(R) = 2\int_R^{R_{max}} n_0\left[1 + ar^{-\gamma}\right] r\left(r^2 - R^2\right)^{-1/2} dr \tag{23.14}$$

The first term of this expression integrates to a constant offset. The second term is complicated, but if $R_{\max} \longrightarrow \infty$, then

$$N(R) \propto R^{1-\gamma} \tag{23.15}$$

Thus, a spatial correlation function which is a power law will produce an angular correlation function that is also a power law, with an exponent that differs by one.

Results from the Two-Point Correlation Function

The results of various galaxy surveys show that the two-point correlation function for galaxies is approximately a power law in the range 0.1 Mpc $< r <$ 16 Mpc, with

$$\xi(r) \sim (r/r_0)^{-\gamma} \tag{23.16}$$

and $\gamma \sim 1.75$. The value of r_0 is called the correlation length. For $r < r_0$, $\xi(r)$ is positive, hence galaxies are clustered on smaller scales. For $r > r_0$, $\xi(r) < 0$, implying a deficit of galaxies in this range. Observations indicate that $r_0 \sim 6h^{-1}$ Mpc. Interestingly, the correlation function for galaxies, galaxy groups, and rich clusters all have approximately the same power-law index. The only difference is their correlation lengths.

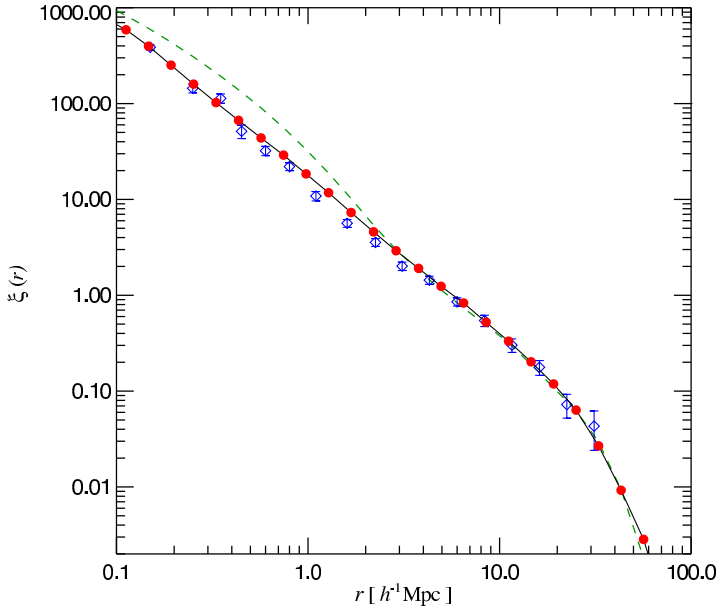

Figure 4: Galaxy 2-point correlation function at the present epoch. Red symbols (with vanishingly small Poisson error-bars) show measurements for model galaxies brighter than $M_K = -23$. Data for the large spectroscopic redshift survey 2dFGRS[28] are shown as blue diamonds. The SDSS[34] and APM[31] surveys give similar results. Both, for the observational data and for the simulated galaxies, the correlation function is very close to a power-law for $r \leq 20h^{-1}$Mpc. By contrast the correlation function for the dark matter (dashed line) deviates strongly from a power-law.

[Springel *et al.* 2005, *Nature*, **435**, 629]

The Correlation Correlation in Fourier Space

Rather than work in terms of ξ, one frequently wants to know how much clustering there is at a given linear scale length. This is given by the Fourier transform of the correlation function, $P(k)$, where k is the wavenumber of the fluctuation (*i.e.*, $2\pi/\lambda$). The two are related via

$$P(k) = \frac{1}{V}\int_0^\infty \xi(r)\frac{\sin kr}{kr}\,4\pi r^2 dr \tag{23.17}$$

and

$$\xi(r) = \frac{V}{2\pi^2}\int P(k)\frac{\sin kr}{kr}k^2 dk \tag{23.18}$$

In this form, we can express the correlation function and density fluctuation in terms of mass. First, we note that if the initial spectrum of fluctuations had no preferred scale, then the simpliest form for the power spectrum would be a power law,

$$P(k) \propto k^n \tag{23.19}$$

If we put this in (23.18), then

$$\xi(r) \propto \int_0^\infty \frac{\sin kr}{kr}k^{n+2}dk \tag{23.20}$$

We can quickly estimate this integral by noting that when $kr \gg 1$, the integrand rapidly goes to zero. Moreover, when $kr \ll 1$, $\sin kr/kr \sim 1$. So to first order

$$\xi(r) \propto \int_0^{1/r} k^{n+2}dk \propto k^{n+3}\Big|_0^{1/r} \propto r^{-(n+3)} \tag{23.21}$$

Since $\mathcal{M} \propto \rho\, r^3$,

$$\xi(\mathcal{M}) \propto \mathcal{M}^{-(n+3)/3} \tag{23.22}$$

Moreover, since ξ has already been associated with the root mean square of a density fluctuation via (23.07), the mass spectrum of density perturbations should be

$$\left(\delta^2_{\mathcal{M}}\right)^{1/2} = A\mathcal{M}^{-(n+3)/6} \tag{23.23}$$

where A is just some constant of proportionality.

Growth of Structure

At the time of the Big Bang, the universe was extremely smooth, but today it is extremely clumpy. How did we get to this state?

First, let's define two classes of perturbations. *Isothermal perturbations* are fluctuations that affect the matter of the universe, but not the surrounding radiation field. These are the types of fluctuations that occur today, since matter and radiation are decoupled. But in the early universe (in the era before recombination), this type of fluctuation may not have existed.

The second class of perturbations are called *adiabatic perturbations.* These effect both light and matter together. Such perturbations do not occur today, but they might have occurred at early times before decoupling.

Isothermal Perturbations

Fluctuations grow due to gravity; the gravitational force per unit mass is

$$F_{\rm grav} = \frac{G\mathcal{M}}{R^2} = \frac{4}{3}\pi G\rho R \tag{23.24}$$

Now consider an isothermal perturbation, where gravity is attempting to move electrons (and protons) through a radition field. The velocity of the electrons is v; the cross section of the electrons to photon absorption is σ_T (the Thomson cross section). Because the electrons are moving through a medium filled with photons, they will experience a drag force. Since the protons must follow the electrons, they will also (indirectly) feel this force. Per unit mass, the drag force is

$$F_{\rm drag} = \frac{aT^4\,(\sigma_T v)}{m_H c} \tag{23.25}$$

(It's not difficult to see where this equation comes from: aT^4 is the energy density (ergs/cm^3) of the microwave background, and $\sigma_T v$ is the cylindrical volume swept out by the electron each second. So the numerator is the amount of energy encountered by the electron each second as it plows through the photons.)

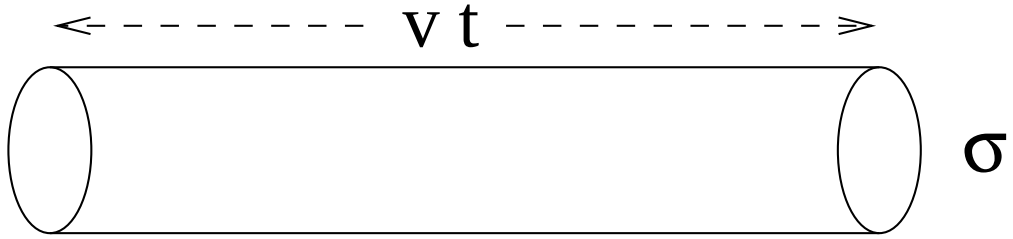

Now, since the universe is expanding and photons are being redshifted,

$$T = T_0(1+z) \qquad \rho = \rho_0(1+z)^3 \tag{23.26}$$

If we compare $F_{\rm drag}$ to $F_{\rm grav}$, and explicity put in the these dependencies, then

$$\frac{F_{\rm drag}}{F_{\rm grav}} = \frac{3\sigma_T v a T^4}{4\pi G m_H c R \rho} = \frac{3\sigma_T v a T_0^4 (1+z)^4}{4\pi G m_H c R \rho_0 (1+z)^3} \tag{23.27}$$

Now consider R, the physical size of the perturbation being considered. In an Einstein de-Sitter universe, the time it takes an electron to move a distance R is approximately vt. If perturbations begin at the time of Big Bang, then by redshift z, the size is

$$R = \frac{2}{3}\frac{1}{H_0} v (1+z)^{-3/2} \tag{23.28}$$

If we use this to substitute for R, then

$$\frac{F_{\rm drag}}{F_{\rm grav}} = \frac{9\sigma_T a T_0^4 H_0}{8\pi G m_H c \rho_c \Omega_0} (1+z)^{5/2} \tag{23.29}$$

Numerically, this works out to be

$$\frac{F_{\rm drag}}{F_{\rm grav}} \sim 10^{-8} (1+z)^{5/2} \tag{23.30}$$

Decoupling occurred at $z \sim 1500$. Before this time, $F_{\rm drag} > F_{\rm grav}$, so gravity could not overcome the drag force of the thermal background. So isothermal perturbations did not grow during this era.

Adiabatic Perturbations

If the radiation field is perturbed along with the matter, the excess energy contained in a region will diffuse outward and damp out the fluctuation. However, this damping does not occur instantaneously.

Let $\lambda = 1/(n_e \sigma_T)$ be the mean free path of a photon. In terms of λ, the time between scatterings for photons is λ/c, and, from statistics, the number of scatterings necessary for a photon to random walk a distance R isa $(R/\lambda)^2$. For a fluctuation *not* to be damped out, the diffusion time must be longer than the age of the universe, *i.e.,*

$$\left(\frac{R}{\lambda}\right)^2 \left(\frac{\lambda}{c}\right) > \frac{2}{3}\frac{1}{H_0}\,(1+z)^{-3/2} \implies R^2 > \frac{2}{3}\frac{c\lambda}{H_0}\,(1+z)^{-3/2} \tag{23.31}$$

Now if we substitute mass for radius and again note that the protons must follow the electrons, so that $\rho = n_e m_H$, then the condition for perturbation growth is

$$\mathcal{M} = \frac{4}{3}\pi\rho R^3 > \frac{4}{3}\pi\rho \left\{\frac{2cm_H}{3H_0\rho\sigma_T}(1+z)^{-3/2}\right\}^{3/2} \tag{23.32}$$

or, if we use (23.26) to substitute for density,

$$\mathcal{M} > \frac{4\pi}{3}\left\{\frac{2cm_H}{3H_0\sigma_T}\right\}^{-3/2}\left\{\frac{1}{\rho_c\Omega_0}\right\}^{1/2}(1+z)^{-15/4} \tag{23.33}$$

where ρ_c is the critical density of the universe. At decoupling, this works out to $M > 10^{13}\mathcal{M}_\odot$. This is somewhat of an underestimate, since λ is changing rapidly in the early universe. But it does demonstrate that adiabatic perturbations can only propagate if they are very large; small scale perturbations will be damped out.

The Jeans Mass

Another question we can ask concerns the minimum mass for gravitational collapse. For collapse to occur, the gravitational potential energy must overcome the thermal motion of the gas. If v_s is the sound speed,

$$\frac{G\mathcal{M}}{R} > \frac{1}{2}v_s^2 \tag{23.34}$$

If we substitute density for radius, then

$$2G\mathcal{M}\left(\frac{4\pi\rho}{3\mathcal{M}}\right)^{1/3} > v_s^2 \tag{23.35}$$

so

$$\mathcal{M}_J = \frac{1}{4}\left(\frac{3}{2\pi}\right)^{\frac{1}{2}} G^{-\frac{3}{2}}\rho^{-\frac{1}{2}}v_s^3 \tag{23.36}$$

where $\mathcal{M}_J$ is called the Jeans mass. After decoupling, matter acted as an ideal gas, so

$$v_s = \left(\frac{\gamma P}{\rho}\right)^{1/2} = \left(\frac{\gamma kT}{m_H}\right)^{1/2} \tag{23.37}$$

If we plug in the numberes for the universe shortly after decoupling, *i.e.*, $z \sim 1000$, then $v_s \sim 4$ km s^{-1}, and the Jeans mass is $\mathcal{M}_J \sim 10^5\mathcal{M}_\odot$. This is similar to the mass of a globular cluster.

In the early universe, however, the ideal gas law did not apply. At $z \sim 40,000$, radiation pressure dominated, and the energy density was much greater than the matter density. So

$$P = \frac{aT^4}{3} \quad \text{and} \quad \rho = \frac{aT^4}{c^2} \tag{23.38}$$

During this time, the sound speed was $v_s \sim c/\sqrt{3}$, and the density was

$$\rho = \frac{a}{c^2} T_0^4 (1+z)^4 \tag{23.39}$$

The Jeans mass was therefore $\mathcal{M}_J \sim 10^{16} \mathcal{M}_\odot$. Again, this demonstrates that large fluctuations could grow in the early universe.

Growth of Perturbations

Can we connect the structure we see today to perturbations in the microwave background? The largest structures in today's universe are superclusters; these have overdensities of $\delta\rho/\rho \sim 2$. To see what that means, consider a region of slightly enhanced density, $\delta\rho$, within an Einstein de-Sitter universe. Recall from our discussion of the basic equations of cosmology (2.02), the expansion of any region of space is given by

$$\left(\frac{\dot{R}}{R}\right)^2 - \frac{8}{3}\pi G(\rho + \delta\rho) = -\frac{kc^2}{R^2} + \frac{\Lambda c^2}{3} \tag{23.40}$$

which, for $\rho > \rho_c$, has the solution,

$$R = a(1 - \cos\theta) \qquad t = \frac{a}{c}(\theta - \sin\theta) \tag{23.41}$$

Let's just consider the R part of the solution. In the early universe, θ was small, so we can Taylor expand the trignometric terms as

$$\cos\theta = 1 - \frac{1}{2}\theta^2 + \frac{1}{24}\theta^4 + \ldots \tag{23.42}$$

So (23.41) becomes

$$R = a\left(\frac{1}{2}\theta^2 - \frac{1}{24}\theta^4 + \ldots\right) \tag{23.43}$$

If we assume the perturbation is small and neglect the higher order terms, then

$$R + \delta R = a\left(\frac{1}{2}\theta^2 - \frac{1}{24}\theta^4\right) \tag{23.44}$$

so

$$R \propto \theta^2 \text{ and } \delta R \propto \theta^4 \Longrightarrow \frac{\delta R}{R} \propto \theta^2 \propto R \tag{23.45}$$

Now let's relate this to the density.

$$\rho = \frac{\mathcal{M}}{R^3} \Longrightarrow \delta\rho = -\frac{3\mathcal{M}}{R^4}\delta R = -\frac{3\rho}{R}\delta R \tag{23.46}$$

so

$$\frac{\delta\rho}{\rho} = 3\frac{\delta R}{R} \tag{23.47}$$

or

$$\frac{\delta\rho}{\rho} \propto \frac{\delta R}{R} \propto R \propto (1+z)^{-1} \tag{23.48}$$

In other words, the amplitude of a small density perturbation will grow linearly with the size of the universe due to the Hubble expansion. This puts a limit on the amplitude of the initial density perturbations: for example, if a supercluster now has $\delta\rho/\rho \sim 2$, at decoupling, the initial density fluctuation must have been at least 1000 times smaller.

Note, however, that very early on, when the universe was dominated by radiation, so $\rho \propto R^4$ (since the dominate source of matter ter/energy was being redshifted). So at this time

$$\frac{\delta\rho}{\rho} \propto R^2 \tag{23.49}$$

One can relate these to time, t in the matter dominated era by (1.29)

$$\frac{\delta\rho}{\rho} \propto R \propto t^{2/3} \tag{23.50}$$

At earlier times, when radiation pressure was important, R went as $t^{1/2}$ (that's an exercise to the student), and

$$\frac{\delta\rho}{\rho} \propto R^2 \propto t \tag{23.51}$$

Press-Schechter Mass Function

[Press & Schechter 1974, *Ap. J.*, **187,** 425]
[Longair 2008, *Galaxy Formation*]

According to CDM scenarios, galaxies and clusters were built via hierarchical clustering. A standard analytical treatment of this process was presented by Press & Schechter in 1974. Although their analysis assumed a critical density universe with no cosmological constant, no dark matter, and neglected a host of very important effects, its result is very close to that predicted by the largest, most modern N-body simulations.

Assume that the primordial density perturbations were randomly distributed in a Gaussian manner. There were just as many positive fluctuations as negative fluctuations, and the probability of a given fluctuation with total mass $\mathcal{M}$ being over (or under) dense by an amplitude $\delta_{\mathcal{M}} = (\rho - \rho_0)/\rho_0$ was

$$p(\delta_{\mathcal{M}}) = \frac{1}{\sqrt{2\pi}\sigma(\mathcal{M})} \exp\left[-\frac{\delta_{\mathcal{M}}^2}{2\sigma^2(\mathcal{M})}\right] \tag{23.52}$$

Obviously, since the fluctuations are Gaussian, the mean-square fluctuation

$$\langle \delta_{\mathcal{M}}^2 \rangle = \sigma^2(\mathcal{M}) \tag{23.53}$$

(This is the same description as for the correlation function, except now we are studying δ as a function of mass, rather than distance.) It is also obvious that before collapse, the volume encompassing this perturbation was related to the mean density of the background by $\mathcal{M} = \rho_0 V$. Now assume that once a perturbation develops an amplitude greater than a critical amplitude δ_c, it evolves rapidly into a bound structure of mass $\mathcal{M}$. (This conveniently neglects all the messy physics of the situation.) For

a fluctuation with a given mass, the fraction of objects that will become bound at a particular epoch is

$$F(\mathcal{M}) = \frac{1}{\sqrt{2\pi}\sigma(\mathcal{M})}\int_{\delta_c}^{\infty}\exp\left[-\frac{\delta^2}{2\sigma^2(\mathcal{M})}\right]d\delta = \frac{1}{2}[1-\mathrm{erf}(t)] \tag{23.54}$$

where $t = \delta_c/\sqrt{2}\sigma(\mathcal{M})$ and erf is the error function. Now recall that the mass spectrum of density perturbations should be

$$\left(\delta^2_{\mathcal{M}}\right)^{1/2} = A\mathcal{M}^{-(n+3)/6} \tag{23.23}$$

so, if we combine this with (23.53), we get

$$\sigma(\mathcal{M}) = \left(\delta^2_{\mathcal{M}}\right)^{1/2} = A^{1/2}\mathcal{M}^{-(n+3)/6} \tag{23.55}$$

So

$$t = \frac{\delta_c}{\sqrt{2}\sigma(\mathcal{M})} = \frac{\delta_c}{\sqrt{2}A^{1/2}}\mathcal{M}^{(3+n)/6} = \left(\frac{\mathcal{M}}{\mathcal{M}^*}\right)^{(3+n)/6} \tag{23.56}$$

where we have replaced δ_c with a reference mass $\mathcal{M}^*$

$$\mathcal{M}^* = \left(\frac{2A}{\delta_c^2}\right)^{3/(3+n)} \tag{23.57}$$

The space density of these perturbations is given by

$$N(\mathcal{M})d\mathcal{M} = \frac{1}{V}\frac{dF(\mathcal{M})}{d\mathcal{M}}d\mathcal{M} = -\left(\frac{\rho_0}{\mathcal{M}}\right)\frac{dF(\mathcal{M})}{d\mathcal{M}}d\mathcal{M} \tag{23.58}$$

(The minus sign comes from our convention – the density of bound structures is inversely dependent on their mass.) Solving for this using (23.54) yields

$$N(\mathcal{M}) = \frac{1}{2\sqrt{\pi}}\left(1+\frac{n}{3}\right)\frac{\rho_0}{\mathcal{M}^2}\left(\frac{\mathcal{M}}{\mathcal{M}^*}\right)^{\frac{(3+n)}{6}}\exp\left[-\left(\frac{\mathcal{M}}{\mathcal{M}^*}\right)^{\frac{(3+n)}{3}}\right] \tag{23.59}$$

All we need now is an estimate of how $\mathcal{M}^*$ changes with time (or redshift). For an Einstein-de Sitter universe, perturbations grow as the size of the universe, R, so

$$\delta_c \propto R \propto t^{2/3} \Longrightarrow \ \langle \delta_c^2 \rangle = \sigma^2(\mathcal{M}) = A\mathcal{M}^{-(3+n)/3} \propto t^{4/3} \tag{23.60}$$

Therefore

$$\mathcal{M}^* \propto A^{3/(3+n)} \propto t^{4/(3+n)} \tag{23.61}$$

or

$$\mathcal{M}^* = \mathcal{M}_0^* \left(\frac{t}{t_0} \right)^{4/(3+n)} \tag{23.62}$$

where $\mathcal{M}_0^*$ is the value of $\mathcal{M}^*$ at the present epoch, t_0. Thus, for a given n, we have a prescription for the number of bound objects of a given mass versus redshift. For reference, the canonical value of n is that proposed by Harrison (1970) and Zel'dovich (1972), $n = 1$.

There are many, many problem with the Press-Schechter formulation (too many to describe here). It neglects peak superpositions (where one falls on top of another), assumes all objects are spherical, and ignores the fact that once structures begins to form, non-linear dynamics will begin to dominate. Nevertheless, it does a remarkably good job a number of observations. For example, note the form of the function: at the high-mass end, there is an exponential cutoff (with the power of $\mathcal{M}/\mathcal{M}^*$ close to one), at low masses, the distribution predicts a power law. This is exactly the form of the Schechter luminosity function.

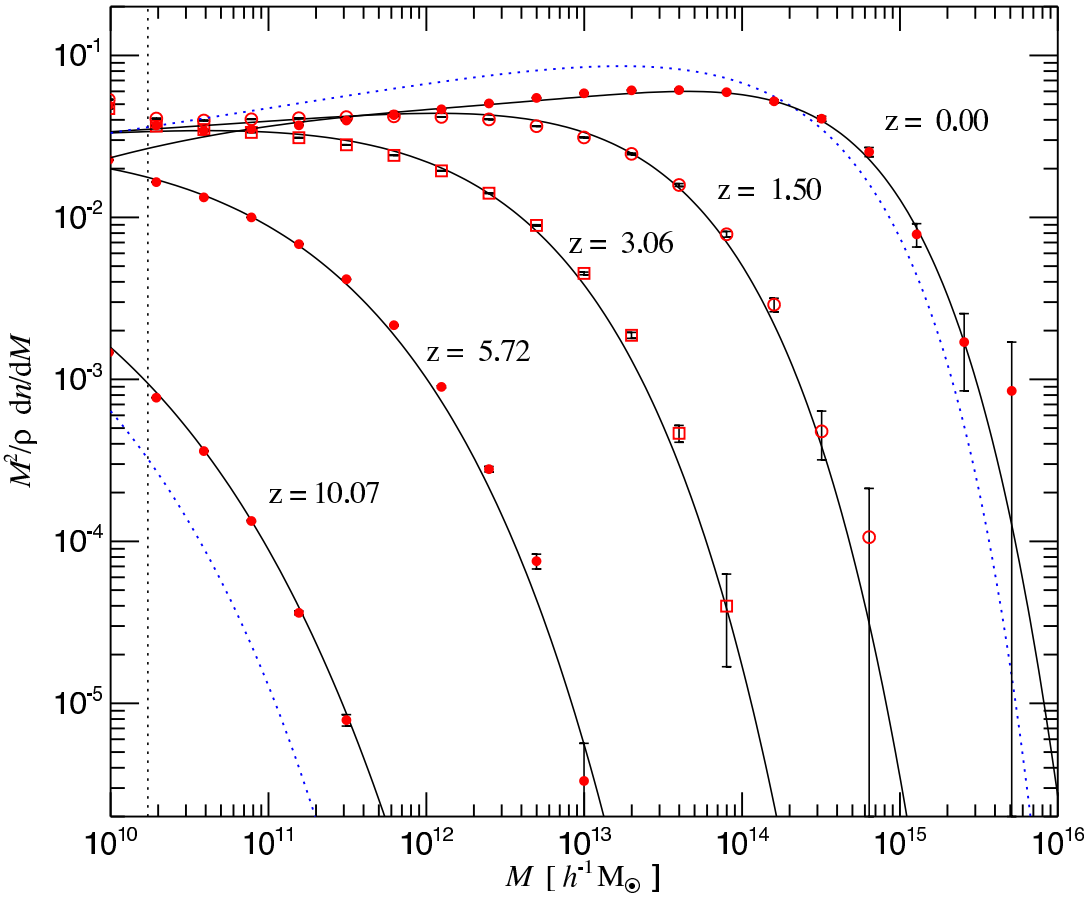

Figure 2: Differential halo number density as a function of mass and epoch. The function $n(M,z)$ gives the comoving number density of halos less massive than M. We plot it as the halo multiplicity function $M^2\rho^{-1}\mathrm{d}n/\mathrm{d}M$, where ρ is the mean density of the universe. Groups of particles were found using a friends-of-friends algorithm[6] with linking length equal to 0.2 of the mean particle separation. The fraction of mass bound to halos of more than 20 particles (vertical dotted line) grows from 6.42×10^{-4} at $z=10.07$ to 0.496 at $z=0$. Solid lines are predictions from an analytic fitting function proposed in previous work[11], while the dashed lines give the Press-Schechter model[14] at $z=10.07$ and $z=0$.

Millenium simulation versus Press-Schechter formulation

[Springel *et al.* 2005, *Nature*, **435**, 629]

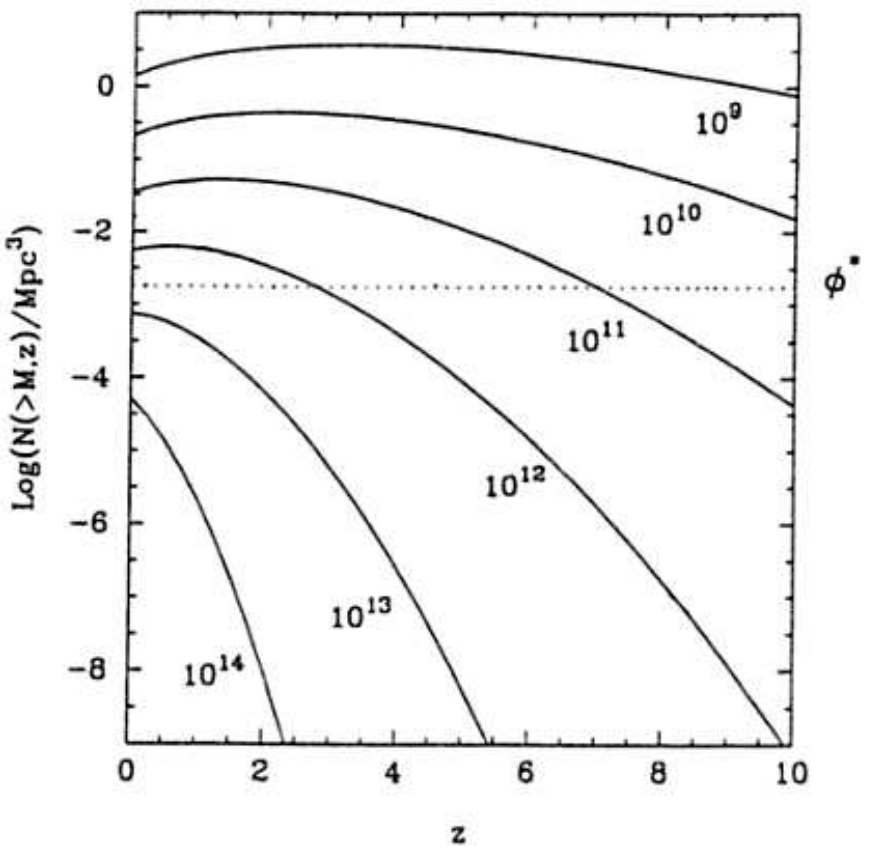

Fig. 16.5 The evolution of the comoving number density of dark matter haloes with masses greater than M as a function of redshift for a standard Cold Dark Matter model with $\Omega_0 = 1$. The curves have been derived using the Press-Schechter form of evolution of the mass spectrum which is a good fit to the results of N-body simulations. The dotted line labelled ϕ^* shows the present number density of L^* galaxies. (after Efstathiou 1995).